A Journal of the Gesellschaft Deutscher Chemiker

Angewandte International Edition GDCh Chemie

www.angewandte.org

Accepted Article

Title: Production of Piperidine and δ-Lactam Chemicals from Biomass-Derived Triacetic Acid Lactone

Authors: Bingfeng Chen, Zhenbing Xie, Fangfang Peng, Shaopeng Li, Junjuan Yang, Tianbin Wu, Honglei Fan, Zhaofu Zhang, Minqiang Hou, Shumu Li, Huizhen Liu, and Buxing Han

To be cited as: *Angew. Chem. Int. Ed.* 10.1002/anie.202102353

Link to VoR: https://doi.org/10.1002/anie.202102353

WILEY-VCH

10.1002/anie.202102353

WILEY-VCH

COMMUNICATION

Production of Piperidine and δ-Lactam Chemicals from Biomass-Derived Triacetic Acid Lactone

Bingfeng Chen,[a] Zhenbing Xie,[a,b] Fangfang Peng,[a] Shaopeng Li,[a] Junjuan Yang,[a] Tianbin Wu,[a] Honglei Fan,[a] Zhaofu Zhang,[a] Minqiang Hou,[a] Shumu Li,[a] Huizhen Liu,*[a,b] Buxing Han*[a,b]

[a] Dr. B. Chen, Z. Xie, F. Peng, S. Li, J. Yang, T. Wu, H. Fan, Z. Zhang, M. Hou, S. Li, Prof. H. Liu, Prof. B. Han
Beijing National Laboratory for Molecular Sciences, CAS Key Laboratory of Colloid, Interface and Chemical Thermodynamics, Institute of chemistry, Chinese Academy of Sciences, Beijing, 100190 (P. R. China)
E-mail: liuhz@iccas.ac.cn; hanbx@iccas.ac.cn.
[b] Prof. H. Liu, Prof. B. Han
School of Chemistry and Chemical Engineering, University of Chinese Academy of Sciences, Beijing, 100049 (P. R. China)

Supporting information for this article is given via a link at the end of the document.((Please delete this text if not appropriate))

Abstract: Piperidine and δ-Lactam chemicals have wide application, which are currently produced from fossil resource in industry. Production of this kind of chemicals from lignocellulosic biomass is of great importance, but is challenging and the reported routes give low yield. Herein, we demonstrate the strategy to synthesize 2-methyl piperidine (**MP**) and 6-methylpiperidin-2-one (**MPO**) from biomass-derived triacetic acid lactone (**TAL**) that is produced microbially from glucose. In this route, **TAL** was firstly converted into 4-hydroxy-6-methylpyridin-2(1H)-one (**HMPO**) through facile aminolysis, subsequently **HMPO** was selectively transformed into **MP** or **MPO** over Ru catalysts supported on beta zeolite (Ru/BEA-X, X is the molar ratio of Si to Al) *via* the tandem reaction. It was found that the yield of **MP** could reach 76.5% over Ru/BEA-60 in *t*-BuOH, and the yield of **MPO** could be 78.5% in dioxane. Systematic studies reveal that the excellent catalytic performance of Ru/BEA-60 was closely correlated with the cooperative effects between active metal and acidic zeolite with large pore geometries. The related reaction pathway was studied on the basis of control experiments.

Valorization of abundant renewable biomass resources provides a prominent strategy for reducing the carbon-footprint of fuels and chemical productions, which primarily rely on dwindling fossil resources. Triacetic acid lactone (**TAL**), which can be produced from glucose *via* efficient polyketide bio-synthesis,[1] is widely utilized in organic synthesis,[2] medicinal chemistry[3] and polymer modifier.[1e,4] However, little attention has been devoted to producing valuable nitrogenous compounds from bio-derived **TAL**.

Pyridine and its derivatives are vital compounds in chemical and bio-chemical industries with an annual production of 375 000 tons in 2018. 2-Methyl piperidine (**MP**), as an important saturated derivative of pyridine,[5] can be used as liquid organic hydrogen carriers,[6] carbon dioxide absorbent[7], building blocks of piperidine alkaloids,[8] and for production of 2-methylpyridine through dehydrogenation. The conventional routes for pyridine and 2-methylpyridine production are still overwhelmingly dependent on fossil resources, including tedious separation procedure from coal tar, reaction of ammonia with aldehydes (formaldehyde, acetaldehyde or acrolein), and the condensation of ammonia or ammonia derivatives with aldehydes, ketones, or α, β-unsaturated carbonyl compounds.[9] Recently, sustainable production of pyridine chemicals from renewable biomass resource has attracted much attention because it provides an eco-friendly alternative to the conventional routes to meet the increasing demands. Pyridine or other nitrogenous heterocyclic compounds can be produced through hydrothermal treatments of renewable raw materials (like cellulose, glycerol, polylactic acid or chitin monomers) with NH_3,[10,11] however, the efficiency was very low with <30% yields of the target products. δ-Lactams, such as 6-methylpiperidin-2-one (**MPO**) and 2-piperidone, are also important structural motifs in the pharmaceutical chemicals, natural products and functional polymers.[12] Although many procedures have been reported on the synthesis of δ-Lactams from fossil raw materials,[13] there is a lack of sustainable route for δ-Lactams production through biomass upgrading.

TAL containing 6-ring building block is an attractive raw material for the production of pyridine. However, the presence of multiple functional groups in its structure often involves hydrogenation, dehydration, ring-opening and decarboxylation.[14,15] Thus, steering reaction pathway toward the desired product remain challenging. Tandem catalysis that enables multistep cascade reactions in a single reactor holds great promise for improving efficiency of biomass upgrading without laborious separation and purification the intermediates,[16] which have been recently reported in the pyrrole production from biomass feedstocks through cascade decarbonylation-amination reaction or hydrogenation-condensation reaction.[17]

Herein, we developed a novel tandem catalytic route with 100% carbon economical route for production of **MP** and **MPO** from biomass-derived **TAL** through 4-hydroxy-6-methylpyridin-2(1H)-one (**HMPO**) as platform. The multi-functional Ru/BEA catalyst can efficiently mediate the tandem reactions, which involves sequential reactions including hydrogenation, dehydration and,

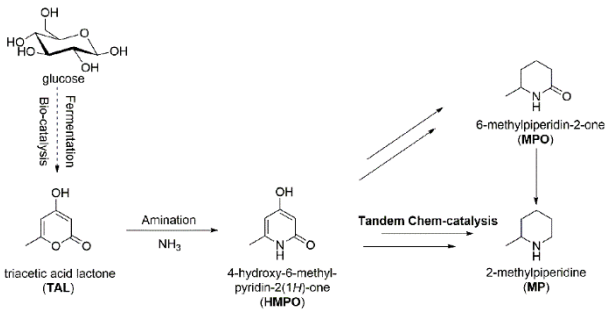

Scheme 1. The proposed reaction pathway for 2-methypiperidine (**MP**) and 6-methylpiperidin-2-one (**MPO**) synthesis from the biomass-derived **TAL**.

hydrodeoxygenation of amide (Scheme 1). The metal and acid sites in Ru/BEA synergistically catalyzed the cascade reaction, and high yields of the products were obtained. To our knowledge, this is the first report on highly efficient routes for the synthesis of piperidine and δ-lactam chemicals from renewable biomass resource.

Firstly, **TAL** was converted into **HMPO** through the direct aminolysis with ammonia, and the preparation procedure was shown in supporting information (Fig. S1).[18] Then, the catalytic transformation of **HMPO** to **MP** was performed over different catalysts. The Ru/BEA-X (X represented the molar ratio of Si to Al) catalysts were prepared by the ion-exchange method. The catalytic performances of Ru/BEA were initially evaluated for the hydrogenation **HMPO** to **MP** using *t*-BuOH as solvent. Ru/BEA-20 gave 33.5% yield of **MP** accompanying with 9.5% yield of **MPO** (Fig. 1). As increasing the Si/Al ratios from 20 to 60 in the BEA support, **MP** yields increased. However, further increasing the Si/Al ratio led to decrease of **MP** yield [Ru/BEA-360] (Fig. 1). The Ru/BEA-60 catalyst achieved the best result with 59.8% yield of **MP** and 11.0% yield of **MPO**. The Ru nanoparticle size distributions over different BEA supports were investigated by TEM analysis (Fig S6), suggesting that the difference in the catalytic performance of the catalyst was not originated mainly from the size effect of Ru particles. To our delight, an excellent yield of 76.5% **MP** was obtained at 200 ^{o}C (Fig. 1). Moreover, the Ru-based catalyst also displayed higher **MP** yield than other supported group VIII metal catalysts (Table S1). Various carbon-supported noble metal catalysts, such as Ru/C, Pd/C and Pt/C, gave low yields of **MP** (Fig. 1 and Table S1). The activity of various oxides supported Ru catalysts were also investigated. It is worth noting that acidic oxides (Al_2O_3 or ZrO_2) supported Ru displayed higher **MP** yields than non-acidic oxide catalysts (SiO_2 or TiO_2) under the same conditions (Fig. 1). Bare BEA zeolite was not active under the identical reaction conditions (Table S1). Compared with Ru/C catalyst, the physical mixture Ru/C and BEA-60 showed an almost two-fold yield of the **MP** (Fig. 1), highlighting the cooperative effect between the active metal and the acidic zeolite. Hence, these results imply that the cascade reaction of **HMPO** into **MP** requires bifunctional catalytic sites under these conditions, i.e., the presence of metal sites for hydrogenation or hydrodeoxygenation and acidic sites for dehydration.

The acidity properties of BEA zeolites catalysts were characterized by ^{27}Al-NMR spectra and NH_3-TPD analysis. The ^{27}Al MAS NMR spectra were conducted to determine the coordination and the local structure of Al atoms in the BEA zeolites. The BEA zeolites showed a strong peak located at 55 ppm (Fig. S2), which is assigned to tetrahedrally coordinated Al sites, and a weak peak at 0 ppm [except BEA-360], corresponding to octahedrally coordinated Al sites.[19] The spectra of all BEA zeolites reveal that most of Al species were located in the zeolite tetrahedral framework work positions, generating bridging OH acid centers.[20] In the temperature-programmed desorption of ammonia curves (NH_3-TPD) of Ru/BEA-60, two desorption peaks at 307 ºC and 453 ºC can be ascribed to medium acid and strong acid sites, respectively (Fig. S3). Generally, increasing aluminum content in Ru/BEA (X=20~60) catalysts resulted in enhancing total acidity (Table S2), however, no clear relationship between the total acidity and catalytic properties was observed. It has been reported that tetrahedrally coordinated Al species give rise to

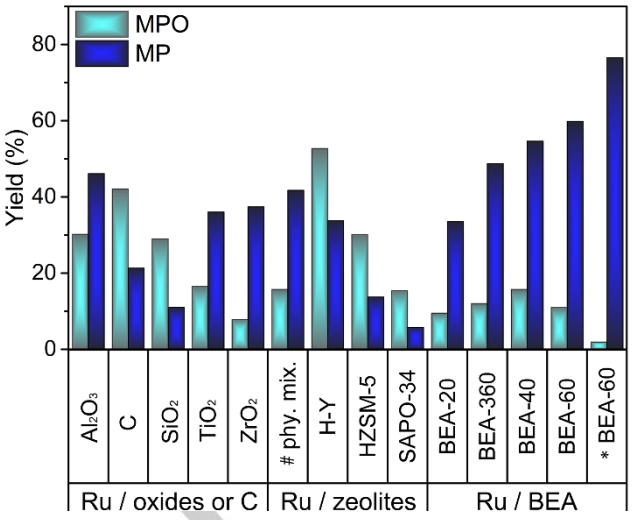

Figure 1. The tandem catalytic transformation of 4-hydroxy-6-methylpyridin-2(1H)-one (**HMPO**) over various heterogeneous catalysts. Reaction conditions: **HMPO** (1 mmol), catalyst (60 mg), *t*-BuOH (2.0 mL), H_2 (5 MPa), 180 ºC/6 h [Yields were determined by GC analysis using dodecane as internal standard; **MPO**: 6-methylpiperidin-2-one; **MP**: 2-methylpiperidine]. # phy. Mix.: Ru/C (60 mg) + BEA-60 (60 mg); * Ru/BEA-60, 200 ºC/6 h.

Bronsted acidic sites, and the extra-framework Al species in BEA zeolites are related to Lewis acidic sites.[21] The former can mediate dehydration reaction in this tandem catalysis, and the latter would be beneficial for the reduction of amide due to interaction between amide and Lewis acidic sites. It has been reported that the catalytic hydrogenation of amide could be improved through activation of carbonyl moiety with Lewis acidic sites in Pt/Nb_2O_5 and Pt-MoO_x/TiO_2 catalysts or V^{3+} species in Pt/V/HAP catalyst.[22] Compared with Ru/BEA-60, Ru/BEA-360 showed a relatively lower yield of **MP** because of less Lewis acidic sites as detected by ^{27}Al-NMR spectra. Details of other characterization results of Ru/BEA catalysts are available in the Supporting Information (Fig. S4-8). Therefore, the excellent performance of Ru/BEA-60 was associated with the suitable acidity of BEA-60 zeolite.

Furthermore, the catalytic performances of other acidic zeolites, such as H-Y, HZSM-5 and SAPO-34, were also investigated in the tandem catalysis. Both Ru/BEA and Ru/H-Y exhibited higher **MP** yields than Ru/HZSM-5 (Fig. 1). This result correlates with the fact that both BEA and H-Y zeolites [12-membered ring (MR) zeolites] possess larger specific surface areas and pore diameters than HZSM-5 (10 MR zeolite). It has been reported that 12-MR zeolites (BEA, MOR) achieved higher catalytic activity than 10 MR zeolite (HZSM-5) in the furfural formation from C_6 sugars owing to diffusion limitations arising from the smaller pore sizes of HZSM-5.[23] Ru/SAPO-34 showed poor performance in the reaction (Fig. 1), which could be associated with diffusional limitation of the product or reagents in the narrow channels of 8 MR SAPO-34 (pore size: ~0.4 nm).[24] Our results show that the catalytic properties were related to types of zeolites, and zeolite topology with large pore size may enhance mass transport. Decarboxylation was not detected in the present catalytic system, indicating preserving carbon skeleton of **TAL**. Ru/BEA-60 was chosen for further investigation, since it exhibited superior catalytic properties compared with others catalysts.

10.1002/anie.202102353

Table 1. The influences of solvents on the catalytic transformation of 4-hydroxy-6-methylpyridin-2(1H)-one (**HMPO**) with Ru/BEA-60 catalyst. [a]

Entry	Solvent	**MPO** Yield (%)[bc]	**MP** Yield (%)[bc]
1	Cyclohexane	32.8	30.1
2	Dioxane	78.5	13.6
3	THF	57.5	18.7
4	*t*-BuOMe[d]	70.1	17.0
5	DME[e]	5.2	-
6	MeOH	8.9	-
7	EtOH	30.8	-
8	1-PrOH	29.0	-
9	2-PrOH	13.4	33.7
10	1-BuOH	29.9	-
11	2-BuOH	2.9	21.6
12	*i*-BuOH[f]	24.5	9.1
13	*t*-BuOH	11.0	59.8
14	1-Pentanol	39.8	-
15	*t*-Pentyl alcohol	44.5	35.0
16	1-Octanol	38.0	14.1

[a] Reaction conditions: **HMPO** (1 mmol), Ru/BEA-60 (Ru: 3.82 wt.%, 60 mg), solvent (2.0 mL), H_2 (5 MPa), 180 ºC/6 h; [b] Yields were determined by GC analysis using dodecane as internal standard; [c] **MPO**: 6-methylpiperidin-2-one; **MP**: 2-methylpiperidine; [d] *t*-BuOMe: *t*-Butyl methyl ether; [e] DME: Dimethoxyethane; [f] *i*-BuOH: 2-Methyl-1-propanol.

The influences of H_2 pressure and temperature on the reaction over Ru/BEA-60 were investigated, and the results were shown in Fig S9 and Fig S10, respectively. The effect of solvent was also examined in the tandem reaction. Non-polar solvent cyclohexane resulted in poor catalytic selectivity and produced almost equivalent amount of **MPO** and **MP** (Table 1, entry 1). Except dimethoxyethane (**DME**), polar aprotic solvents, including dioxane, THF and *t*-butyl methyl ether, all gave **MPO** as the main product (Table 1 entry 2-5). Especially, the yield of **MPO** in dioxane could reach 78.5% (Table 1, entry 2). The performances of polar protic solvents were also studied. The tertiary alcohols gave higher **MP** yields than primary and secondary alcohols (Table 1 entry 6-16), and *t*-BuOH resulted in the best result (Table 1 entry 13).

To get some kinetic information, the time curves of tandem reaction of **HMPO** in *t*-BuOH and dioxane are provided in Fig. S11 and Fig. S12, respectively. The results indicated that **MPO** was first generated in *t*-BuOH, which was converted into **MP** as the principal product with prolonging the reaction time (Fig. S11). Beside **MPO** and **MP**, 4-hydroxy-2-methyl-6-oxopiperidine (**HMOP**) intermediate was also detected at the early stage of the cascade reaction, which was derived from hydrogenation of **HMPO**. These results demonstrate that metal-mediated ring hydrogenation and acid-catalyzed dehydration of **HMPO** dominate the conversion during the first two hours, and subsequent reduction of amide produces **MP**. In dioxane, however, **MPO** was the main product accompanying with **MP** as minor product during all the reaction process (Fig. S12). Taking into account both of Table 1 and Fig. S11-12, it is clear that solvent influences the kinetics of the reaction and the product distribution.

To obtain further mechanistic insight into the tandem catalysis of the biobased **TAL**, several control experiments were conducted over Ru/BEA-60 (Fig. 2). It has been reported that there exists equilibrium between **HMPO** and its enol isomer 2,4-dihydroxy-6-methylpyridine (**DHMP**).[25] The reactivity of **DHMP** was checked, and 34.7% yield of **MP** was obtained. Furthermore, the hydrogenation of **MPO** gave **MP** in 20.6% yield (Fig. 2). **HMOP** was detected by electrospray ionization (ESI) Fourier transform ion cyclotron mass spectrometry (FT-ICR MS) with a m/z of 152.0682 $[M+Na]^+$, which was identified in the tandem catalysis of both **HMPO** and **DHMP** at the initial stage of reaction. On the basis of the above analysis results, the overall reaction route of **MP** production from **TAL** is proposed through **HMPO** as platform (Scheme 2). After the facile aminolysis of **TAL** with ammonia, the reaction route proceeds through a metal-catalyzed hydrogenation of double bonds in the **HMPO**, followed by acid-catalyzed dehydration and metal-catalyzed hydrogenation of amide derivative. Subsequently, the produced amide undergoes deoxygenative hydrogenation to cyclic amine assisting by amide activation with Lewis acidic sites. Therefore, the successfully cascade catalytic transformation of **HMPO** into **MP** was ascribed to the cooperative effects between active metal, Brönsted acid and Lewis acid sites in the multifunctional catalytic systems.

To explore the stability of the multifunctional catalyst, the reusability of Ru-BEA-60 was investigated under the optimal conditions. As shown in Fig. S13, a slight decrease of the yield of **MP** was detected after three cycles. The phase structure, chemical composition and the dispersions of supported Ru nanoparticles for the recycled catalyst did not change obviously compared to the fresh one (Fig. S14). A slight decrease in **MP** yield could be attributed to the inevitable loss of some catalyst during the recovery procedure. These results demonstrate that the Ru-based multifunctional catalyst showed good recyclability in the tandem reaction.

In summary, we demonstrate efficient route to produce **MP** and **MPO** from biomass-derived **TAL**. After facile aminolysis of **TAL**, the selective production of **MP** or **MPO** from **HMPO** requires tandem catalysis. The yield of **MP** reaches 76.5% over the multifunctional Ru/BEA-60 catalyst in *t*-BuOH, superior to the

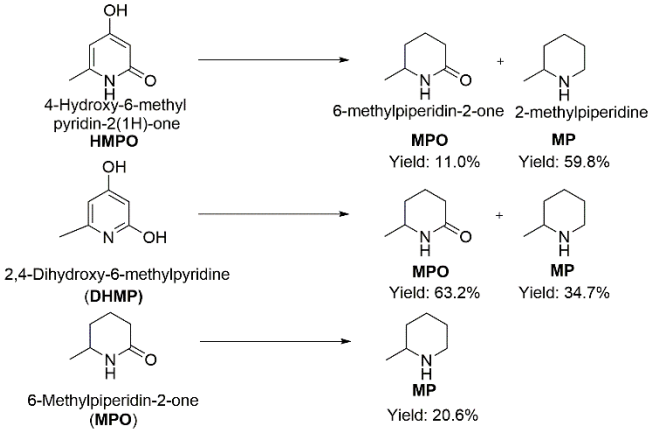

Figure 2. Catalytic conversion of **HMPO**, **DHMP** and **MPO** into lactam and/or piperidine with Ru/BEA-60 catalyst. Reaction conditions: Reactant (1 mmol), Ru/BEA-60 catalyst (Ru: 3.82 wt.%, 60 mg), *t*-BuOH (2.0 mL), H_2 (5 MPa), 180 ºC/6 h.

other zeolites supported catalysts and commercial catalysts. In dioxane, **MPO** is the principal product with a yield of 78.5%. Systematic studies reveal that the excellent catalytic properties of Ru/BEA were closely correlated with the cooperative effects between active metal and acidic zeolite with large pore geometries. This work opens up the way for efficient production of piperidine and δ-lactam chemicals from renewable biomass.

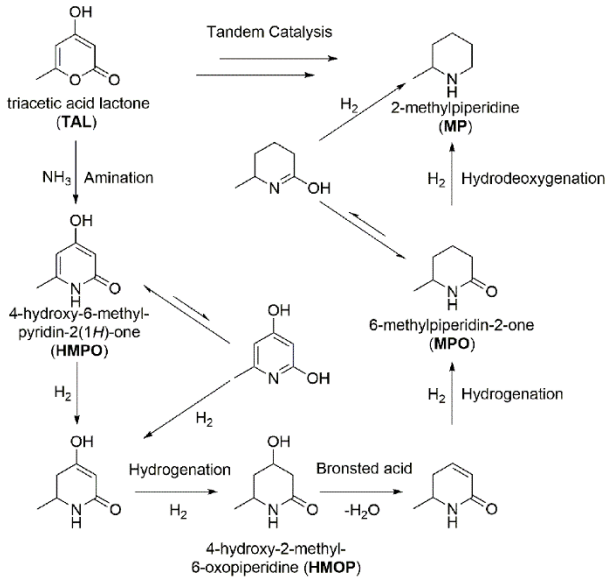

Scheme 2. The proposed reaction pathway for tandem catalysis of biomass-derived **TAL** into 2-methypiperidine (**MP**) and 6-methylpiperidin-2-one (**MPO**) over Ru/BEA catalysts.

Acknowledgements

This work was financially supported by the National Key Research and Development Program of China (2017YFA0403103, 2017YFA0403003), National Natural Science Foundation of China (21871277, 21403248 and 22003069), Beijing Municipal Science & Technology Commission (Z191100007219009), and the Chinese Academy of Sciences (QYZDY-SSW-SLH013).

Keywords: Biomass conversion • N-Heterocycle •Zeolites • Tandem Catalysis • Sustainable chemistry

[1] a) S. Eckermann, G. Schroder, J. Schmidt, D. Strack, R. A. Edrada, Y. Helariutta, P. Elomaa, M. Kotilainen, I. Kilpelainen, P. Proksch, T. H. Teeri, J. Schroder, *Nature* **1998**, *396*, 387-390; b) W. J. Zha, Z. Y. Shao, J. W. Frost, H. M. Zhao, *J. Am. Chem. Soc.* **2004**, *126*, 4534-4535; c) S. Y. Tang, S. Qian, O. Akinterinwa, C. S. Frei, J. A. Gredell, P. C. Cirino, *J. Am. Chem. Soc.* **2013**, *135*, 10099-10103; d) J. Gajewski, F. Buelens, S. Serdjukow, M. Janssen, N. Cortina, H. Grubmuller, M. Grininger, *Nat. Chem. Biol.* **2017**, *13*, 463-465; e) K. A. Markham, C. M. Palmer, M. Chwatko, J. M. Wagner, C. Murray, S. Vazquez, A. Swaminathan, I. Chakravarty, N. A. Lynd, H. S. Alper, *Proc. Natl. Acad. Sci. USA* **2018**, *115*, 2096-2101; f) Z. G. Tan, J. M. Clomburg, S. Cheong, S. Qian, R. Gonzalez, *Nat*. *Catal*. **2020**, *3*, 593-603.

[2] a) D. L. Obydennov, A. I. El-Tantawy, V. Y. Sosnovskikh, *Mendeleev Commun*. **2019**, *29*, 1-10; b) M. Moreno-manas, R. Pleixats, *Advances in Heterocyclic Chemistry* **1992**, *53*, 1-84.

[3] a) B. H. Shanks, P. L. Keeling, *Green Chem*. **2017**, *19*, 3177-3185; b) G. M. Ziarani, R. Moradi, M. Zandiyeh, N. Lashgari, *Heterocycles* **2018**, *96*, 381-424.

[4] H. Sajjad, W. B. Tolman, T. M. Reineke, *ACS Appl. Polym. Mater.* **2020**, *2*, 2719-2728.

[5] a) A. R. Katritzky, C. A. Ramsden, J. A. Joule, V. V. Zhdankin in *Handbook of heterocyclic chemistry*, Elsevier, Netherlands, **2010**, pp. 18-19; b) F. W. Fowler in *Comprehensive Heterocyclic Chemistry, Vol. 2* (Ed.: A. R Katritzky, C. W. Rees), Elsevier, **1984**, pp. 365-394.

[6] a) Y. J. Xie, D. Milstein, *ACS Appl. Energy Mater*. **2019**, *2*, 4302-4308; b) H. Yook, K. Kim, J. H. Park, Y. W. Suh, J. W. Han, *Catal*. *Today* **2020**, *352*, 345-353.

[7] a) C. McGregor, M. S. Al-Abdul-Wahid, V. Robertson, J. S. Cox, P. R. Tremaine, *J. Phys. Chem. B* **2018**, *122*, 9178-9190; b) O. Fandino, S. Sasidharanpillai, D. V. Soldatov, P. R. Tremaine, *J. Phys. Chem. B* **2018**, *122*, 10880-10893; c) Y. Coulier, A. Lowe, P. R. Tremaine, J. Y. Coxam, K. Ballerat-Busserolles, *Int. J. Greenh. Gas Con.* **2016**, *47*, 322-329.

[8] a) D. O'Hagan, *Nat. Prod. Rep.* **2000**, *17*, 435-446; b) D. O'Hagan, *Nat. Prod. Rep.* **1997**, *14*, 637-651; c) M. Sugiura, H. Hagio, R. Hirabayashi, S. Kobayashi, *J. Am. Chem. Soc.* **2001**, *123*, 12510-12517.

[9] C. Allais, J. M. Grassot, J. Rodriguez, T. Constantieux, *Chem*. *Rev*. **2014**, *114*, 10829-10868.

[10] a) L. J. Xu, Z. Han, Q. Yao, J. Deng, Y. Zhang, Y. Fu, Q. X. Guo, *Green Chem*. **2015**, *17*, 2426-2435; b) Y. C. Zhang, X. Yan, B. Q. Niu, J. Q. Zhao, *Green Chem*. **2016**, *18*, 3139-3151; c) L. J. Xu, Q. Yao, Z. Han, Y. Zhang, Y. Fu, *ACS Sustainable Chem. Eng.* **2016**, *4*, 1115-1122; d) L. J. Xu, Q. Yao, J. Deng, Z. Han, Y. Zhang, Y. Fu, G. W. Huber, Q. X. Guo, *ACS Sustainable Chem. Eng.* **2015**, *3*, 2890-2899; e) S. Q. Xie, C. H. Jia, S. S. G. Ong, Z. L. Wang, M. J. Zhu, Q. J. Wang, Y. H. Yang, H. F. Lin, *iScience* **2020**, *23*, 101096.

[11] a) H. Li, H. X. Guo, Z. Fang, T. M. Aida, R. L. Smith, *Green Chem*. **2020**, *22*, 582-611; b) Y. Z. Wang, S. Furukawa, X. P. Fu, N. Yan, *ACS Catal*. **2020**, *10*, 311-335; c) L. J. Xu, C. C. Shi, Z. J. He, H. Zhang, M. Y. Chen, Z. Fang, Y. Zhang, *Energ*. *Fuel* **2020**, *34*, 10441-10458.

[12] a) E. Vitaku, D. T. Smith, J. T. Njardarson, *J. Med. Chem.* **2014**, *57*, 10257-10274; b) R. D. Taylor, M. MacCoss, A. D. G. Lawson, *J. Med. Chem.* **2014**, *57*, 5845-5859; c) D. O'Hagan, *Nat. Prod. Rep.* **2000**, *17*, 435-446; d) R. O'Reilly, N. S. Ieong, P. C. Chua, M. A. Kelland, *Chem*. *Eng*. *Sci*. **2011**, *66*, 6555-6560; e) Q. Zhang, I. M. Heyns, R. Pfukwa, B. Klumperman, M. A. Kelland, *Energ*. *Fuel* **2018**, *32*, 12337−12344; f) J. Liu, H. Wang, J. Guo, G. Chen, J. Zhong, Y. Yan, J. Zhang, *J. Nat. Gas Sci. Eng.* **2020**, *83*, 103504; g) H. Y. Kim, J. S. Goh, M. H. Ryu, D. S. Kim, B. K. Song, S. H. Lee, S. J. Park, J. Jegal, *Polymer-Korea* **2014**, *38*, 31-37.

[13] For selected examples, see: a) T. Wagener, L. Luckemeier, C. G. Daniliuc, F. Glorius, *Angew. Chem. Int. Ed.* **2021**, *60*, 6425-6429; b) I. S. Hassan, A. N. Ta, M. W. Danneman, N. Semakul, M. Burns, C. H. Basch, V. N. Dippon, B. R. McNaughton, T. Rovis, *J. Am. Chem. Soc.* **2019**, *141*, 4815−4819; c) X. J. Jin, K. Kataoka, T. Yatabe, K. Yamaguchi, N. Mizuno, *Angew. Chem. Int. Ed.* **2016**, *55*, 7212-7217; d) J. R. Khusnutdinova, Y. Ben-David, D. Milstein, *J. Am. Chem. Soc.* **2014**, *136*, 2998-3001; e) M. Kunishima, K. Hioki, T. Moriya, J. Morita, T. Ikuta, S. Tani, *Angew. Chem. Int. Ed.* **2006**, *45*, 1252-1255; f) N. Tanaka, T. Usuki, *Eur. J. Org. Chem.* **2020**, 5514–5522; g) H. Li, H. G. Wu, H. Zhang, Y. G. Su, S. Yang, E. J. M. Hensen, *ChemSusChem* **2019**, *12*, 3778-3784; h) H. J. Kiely-Collins, I. Sechi, P. E. Brennan, M. G. McLaughlin, *Chem. Commun.* **2018**, *54*, 654-657; i) D. Pingen, D. Vogt, *Catal. Sci. Technol.* **2014**, *4*, 47-52; j) D. Stibal, J. Sa, J. A. van Bokhoven, *Catal. Sci. Technol.* **2013**, *3*, 94-98.

[14] a) M. Chia, T. J. Schwartz, B. H. Shanks, J. A. Dumesic, *Green Chem.* **2012**, *14*, 1850-1853; b) T. J. Schwartz, R. L. Johnson, J. Cardenas, A. Okerlund, N. A. Da Silva, K. Schmidt-Rohr, J. A. Dumesic, *Angew. Chem. Int. Ed.* **2014**, *53*, 12718-12722.

[15] a) M. Chia, M. A. Haider, G. Pollock, G. A. Kraus, M. Neurock, J. A. Dumesic, *J. Am. Chem. Soc.* **2013**, *135*, 5699-5708; b) S. Gupta, M. I. Alam, T. S. Khan, N. Sinha, M. A. Haider, *RSC Adv*. **2016**, *6*, 60433-60445; c) G. Shrivastav, T. S. Khan, M. Agarwal, M. A. Haider, *J. Phys. Chem. C* **2018**, *122*, 11599-11607; d) S. Gupta, M. I. Alam, T. S. Khan, M. A. Haider, *ACS Sustainable Chem. Eng.* **2019**, *7*, 10165-10181; e) C. L. Sun, A. Furstner, *Angew. Chem. Int. Ed.* **2013**, *52*, 13071-13075.

[16] a) M. A. Isaacs, C. M. A. Parlett, N. Robinson, L. J. Durndell, J. C. Manayil, S. K. Beaumont, S. Jiang, N. S. Hondow, A. C. Lamb, D. Jampaiah, M. L. Johns, K. Wilson, A. F. Lee, *Nat*. *Catal*. **2020**, *3*, 921-931; b) X. Y.

10.1002/anie.202102353

Wang, R. Rinaldi, *Angew. Chem. Int. Ed.* **2013**, *52*, 11499-11503; c) L. Bui, H. Luo, W. R. Gunther, Y. Roman-Leshkov, *Angew. Chem. Int. Ed.* **2013**, *52*, 8022-8025; d) H. J. Cho, D. Kim, J. Li, D. Su, B. J. Xu, *J. Am. Chem. Soc.* **2018**, *140*, 13514-13520; e) Y. Song, X. Y. Feng, J. S. Chen, C. Brzezinski, Z. W. Xu, W. B. Lin, *J. Am. Chem. Soc.* **2020**, *142*, 4872-4882; f) M. J. Climent, A. Corma, S. Iborra, M. J. Sabater, *ACS Catal.* **2014**, *4*, 870-891.

[17] a) S. Song, V. F. K. Yuen, L. Di, Q. M. Sun, K. Zhou, N. Yan, *Angew. Chem. Int. Ed.* **2020**, *59*, 19846-19850; b) P. Ryabchuk, T. Leischner, C. Kreyenschulte, A. Spannenberg, K. Junge, M. Beller, *Angew. Chem. Int. Ed.* **2020**, *59*, 18679-18685.

[18] W. Stadlbauer, W. Fiala, M. Fischer, G. Hojas, *J. Heterocyclic Chem.* **2000**, *37*, 1253-1256.

[19] a) M. H. Sun, L. H. Chen, S. Yu, Y. Li, X. G. Zhou, Z. Y. Hu, Y. H. Sun, Y. Xu, B. L. Su, *Angew. Chem. Int. Ed.* **2020**, *59*, 19582-19591; b) J. J. Gabla, S. R. Mistry, K. C. Maheria, *Catal. Sci. Technol.* **2017**, *7*, 5154-5167.

[20] J. Xu, Q. Wang, F. Deng, *Acc. Chem. Res.* **2019**, *52*, 2179-2189.

[21] a) R. Ramos, A. Grigoropoulos, B. Griffiths, A. P. Katsoulidis, M. Zanella, T. D. Manning, F. Blanc, J. B. Claridge, M. J. Rosseinsky, *J. Catal.* **2019**, *375*, 224-233; b) L. Bui, H. Luo, W. R. Gunther, Y. Roman-Leshkov, *Angew. Chem. Int. Ed.* **2013**, *52*, 8022-8025; c) R. Baran, Y. Millot, T. Onfroy, J. M. Krafft, S. Dzwigaj, *Microp. Mesop. Mat.* **2012**, *163*, 122-130.

[22] a) T. Mitsudome, K. Miyagawa, Z. Maeno, T. Mizugaki, K. Jitsukawa, J. Yamasaki, Y. Kitagawa, K. Kaneda, *Angew. Chem. Int. Ed.* **2017**, *56*, 9381-9385; b) K. Shimizu, W. Onodera, A. S. Touchy, S. M. A. H. Siddiki, T. Toyao, K. Kon, *ChemistrySelect* **2016**, *4*, 736-740.

[23] E. I. Gurbuz, J. M. R. Gallo, D. M. Alonso, S. G. Wettstein, W. Y. Lim, J. A. Dumesic, *Angew. Chem. Int. Ed.* **2013**, *52*, 1270-1274.

[24] a) X. Q. Hu, M. Yang, D. Q. Fan, G. S. Qi, J. Wang, J. Q. Wang, T. Yu, W. Li, M. Q. Shen, *J. Catal.* **2016**, *341*, 55–61; b) P. Cnudde, R. Demuynck, S. Vandenbrande, M. Waroquier, G. Sastre, V. Van Speybroeck, *J. Am. Chem. Soc.* **2020**, *142*, 6007-6017; c) P. H. Yan, G. Bryant, M. M. J. Li, J. Mensah, E. Kennedy, M. Stockenhuber, *Micro. Meso. Mater.* **2020**, *309*, 110561.

[25] a) P. Beak, *Acc. Chem. Res.* **1977**, *10*, 186−192; b) H. B. Schlegel, P. Gund, E. M. Fluder, *J. Am. Chem. Soc.* **1982**, *104*, 5347-5351; c) N. Tsuchida, S. Yamabe, *J. Phys. Chem. A* **2005**, *109*, 1974-1980.

10.1002/anie.202102353

WILEY-VCH

COMMUNICATION

Entry for the Table of Contents

Insert graphic for Table of Contents here. ((Please ensure your graphic is in **one** of following formats))

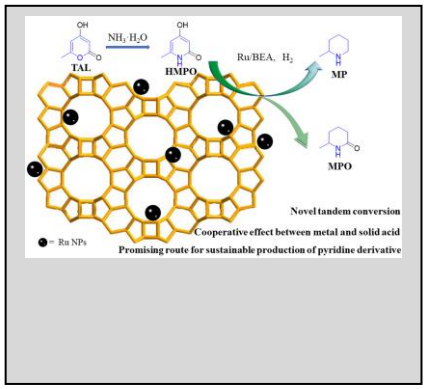

A novel tandem catalytic route was developed for the selective production of 2-methyl piperidine (**MP**) or 6-methylpiperidin-2-one (**MPO**) from biomass-derived triacetic acid lactone (**TAL**), which opens the way for efficient production of piperidine and δ-lactam chemicals from renewable biomass.